IDENTIFYING THE EFFECT OF WIND CONDITION ON CANOPY URBAN HEAT ISLAND

A Case Study in Nanjing

XINYUAN HAO[1]and ZIYU TONG[2]
[1,2]*School of Architecture and Urban Planning, Nanjing University.*
[1]*xinyuan.hao@foxmail.com, 0000-0001-9583-6254*
[2]*tzy@nju.edu.cn, 0000-0002-5872-0890*

Abstract. The canopy urban heat island (CUHI) stands for the phenomenon where the air temperature in an urban area is significantly higher than in a suburban area. Identifying CUHIs and their pattern can improve the health and comfort of urban residents. However, previous studies have focused more on surface urban heat island (SUHI) yet lacking a proper quantification tool for canopy heat islands. This study integrates local climate zone (LCZ), urban form classification data, and anthropogenic heat to quantify the canopy temperature, so as to analyze the distribution of CUHIs as well as the relation with wind condition. The case study of Nanjing selects the weather data representing days with different wind directions, uses WRF to simulate local air temperatures and wind speeds and directions, and analyses the influence of wind on CUHI through comparison. The results show that: 1) in the case of Nanjing, wind direction within 50-90° increases CUHI and leads to a continuous rise in air temperature; 2) when the wind direction falls in some specific ranges, the overall CUHI area significantly shrinks. In short, this paper shows how wind condition affects CUHI, which contributes to predicting CUHI and reducing the risk of heat exposure to urban populations, and provides guidance for urban management and design.

Keywords. Canopy Urban Heat Island (CUHI), Wind Condition, Weather Research and Forecasting (WRF), Local Climate Zone (LCZ).

1. Introduction

As global temperatures rise and extreme heat events occur more frequently, the urban heat island (UHI) phenomenon is increasingly affecting the daily work and lives of urban residents. Urban heat islands can be investigated in two layers: surface urban heat island (SUHI) and canopy urban heat island (CUHI) (Peng et al., 2022). SUHI refers to the phenomenon that surface temperature rises more than suburban, which can be quantified and standardized by land surface temperature (LST) data derived from satellite images. Some factors affect the SUHI intensity, such as the surface

HUMAN-CENTRIC, Proceedings of the 28th International Conference of the Association for Computer-Aided Architectural Design Research in Asia (CAADRIA) 2023, Volume 2, 623-632. © 2023 and published by the Association for Computer-Aided Architectural Design Research in Asia (CAADRIA), Hong Kong.

impermeability and building density (Hu et al., 2019, Zhou et al., 2022). Due to the accessibility of LST data, existing studies have focused mainly on SUHI.

The canopy urban heat island (CUHI) refers to the phenomenon of higher temperatures in the urban canopy compared to the suburbs and is closely related to the air temperature rise above the surface. The characteristics and patterns of CUHIs at both the urban and local scales could be valuable for improving human comfort and health and mitigating the risks of heat exposure to populations on extremely hot days (Li et al., 2023, Thanvisitthpon, 2022). The distribution of CUHIs is affected by local turbulence and the overall ventilation of the city, so it shows great disparities among different locations and exhibits trends of movement (Zheng et al., 2022, He, 2022, Huang et al., 2020). As LST data cannot be used to describe the canopy temperature (the air temperature above the surface) at a particular moment in time, relatively few studies have explored CUHI to date.

This study focuses on the characteristics and patterns of CUHIs at the urban scale, as such CUHIs have been shown to directly influence the health and comfort of urban residents in many studies. Identifying and recognizing CUHIs and their pattern are important to improve the health and comfort of urban residents (Chen et al., 2022, Estoque et al., 2020). Thus accurate canopy temperature data of higher resolution grids and longer time series are required to identify CUHIs. Weather research and forecasting (WRF) is a mesoscale meteorological model used mainly for weather condition prediction and simulation. This model uses open-source, traceable external meteorological data as the boundary field conditions and optional regional geographic data as the initial field conditions (Wang et al., 2019), and its simulation results can be used flexibly to describe air temperatures for identifying CUHIs. In addition, WRF can also provide information on other climate variables such as wind conditions and humidity that may be relevant to CUHIs and their intensity (CUHII). In summary, this study uses the WRF model, combined with suitable urban canopy data, to obtain urban canopy temperature data and the CUHIs distribution at particular moments, and to conduct correlation analyses in conjunction with wind conditions.

2. Methodology

Based on the conclusion that wind conditions and UHI are correlated derived in existing studies (Wang et al., 2020), CUHI and its intensity are assumed to be directly impacted by wind conditions (Xue et al., 2023). Therefore, we set up a control group of weather cases to perform a correlation study between CUHIs and wind conditions, that is, to analyze the changes in wind conditions while controlling for unchanged canopy temperatures. In terms of the technical path, after weather cases with similar overall air temperatures were selected from external data, we obtained different wind conditions and local canopy temperatures under these weather cases through WRF simulations, and then further conducted a correlation analysis between wind conditions and CUHIs while considering the changes of CUHII and the distribution characteristics of the wind directions.

2.1. PREPARATION DATA FOR RESEARCH CASES

The main urban areas of China's large cities have been relatively constant over the last

five years and the urban canopy patterns of these cities could be treated as unchanged. Thus, weather cases with comparative values were selected as the base data for WRF simulations. The high temperature days over the last 5 years were firstly identified from the observatory data, and dates with consistent average daily temperatures were screened; then, moments with similar wind speeds but large differences in wind direction were selected. Then, the external weather data representing specific periods were input into the WRF model to perform simulations. Results containing the main weather variables of concern, such as air temperature and wind conditions, were obtained, thereby composing the comparable weather cases group.

2.2. IDENTIFICATION OF CUHIS AND QUANTIFICATION OF WIND CONDITIONS

We assumed that the air temperature varied from one weather case to another due to the differences in wind conditions and classified CUHIs mainly by the increase in the air temperature. Thus, CUHI could be calculated using the variable T2 in WRF simulation results with the following formula:

$$CUHI_{grid} = T_{grid} - T_{area}$$

where T_{grid} and T_{area} are the temperatures of the specified urban grids and whole study area, respectively; the units of all items are degrees Celsius (°C).

The wind speed and direction are calculated mainly from the x-component and y-component of the wind with the following formula:

$$Speed_{grid} = \sqrt{U10_{grid}{}^2 + V10_{grid}{}^2}$$

$$Angle_{grid} = \begin{cases} \tan^{-1}\dfrac{|U10|}{|V10|} * 180/\pi, & U10 \geq 0 \; and \; V10 \geq 0 \\ 360 - \tan^{-1}\dfrac{|U10|}{|V10|} * 180/\pi, & U10 < 0 \; and \; V10 \geq 0 \\ 180 - \tan^{-1}\dfrac{|U10|}{|V10|} * 180/\pi, & U10 \geq 0 \; and \; V10 < 0 \\ 180 + \tan^{-1}\dfrac{|U10|}{|V10|} * 180/\pi, & U10 < 0 \; and \; V10 < 0 \end{cases}$$

where U10 and V10 are the x-component and y-component of the specified urban grid, respectively; the unit of the speed is m/s, and the unit of the angle is degree (°).

2.3. ANALYSIS OF THE CUHII AND WIND CONDITIONS

The intensity of CUHI (CUHII) in the study area can be classified by natural breakpoint grading method, allowing for more obvious and plausible differences between classes (Lu. et al., 2021, Liang. et al., 2020). In turn, the variation of CUHII among different weather cases can be calculated from the differences among different CUHII classes, using the following formulas respectively:

$$\Delta CUHII_{\mathrm{C}} = CUHII_{\mathrm{case1}} - CUHII_{\mathrm{case2}}$$

where $CUHII_{\mathrm{case1}}$ and $CUHII_{\mathrm{case2}}$ are the CUHI intensities of the specified

urban grids in different cases.

The study area was categorized into three types according to the distribution of the values of $\Delta CUHII_C$: the high CUHII zone existed only in case 1, the high CUHII zone existed only in case 2, or the high CUHII zone existed in both cases. The wind condition characteristics were studied within each zone.

Moreover, since the selected cases had the same average temperature (T_{area}), the difference in the canopy temperature, ΔT_{grid}, was also used to directly describe CUHII changes with the following formula:

$$\Delta T_{grid} = T_{case1} - T_{case2}$$

where T_{case1} and T_{case2} are the temperatures of the specified urban grids in different cases.

We defined the areas with ΔT_{grid} smaller than a certain value as the "main cooling zone", and the areas with ΔT_{grid} higher than a certain value as the "main warming zone". The certain values were determined by the range of temperatures in different cases using the natural breakpoint grading method.

This research focused mainly on the wind directions, including the distribution characteristics, mean value, and standard deviation. Such information helped to summarize the relevance of the wind directions to the CUHIs. In addition, considering the boundary nature of the study area, it was important to pay attention to filtering outliers in the wind conditions data.

3. Case study

3.1. STUDY AREA

The main urban area of Nanjing was chosen as the study area due to its typical extremely hot summers and high-density building environment. Nanjing is located north of 30°N latitude and has a subtropical monsoon climate, with the temperatures peaking in summers and main winds blowing east or southeast. The central six districts feature higher building densities and are divided into two parts by the Yangtze River to the northwest. Thus the SUHI distribution in the study area is patchy, with aggregated non-water surfaces (Figure 1). We obtained data representing the surface skin temperature from the WRF simulation at 12 noon local time on 28 July 2017, and then obtained information subsequently using the natural breakpoint grading method.

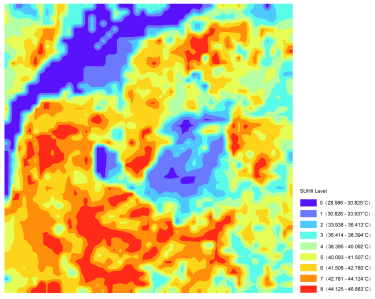

Figure 1. SUHII in the main urban area of Nanjing

The urban form and building density in Nanjing's main urban area has been almost stable over the last five years, based on which we selected moments of similar temperatures but disparate wind conditions in summers: first, the observation data (NO.58283) were used to filter out the high temperature days in Nanjing from 2015 to 2022; second, 17:00 on 24 July 2017 (case 1) and 18:00 on 13 August 2022 (case 2) were selected to form the comparable cases group which have similar wind speeds but different wind directions (Table 1); finally, the near 3-day FNL (Final Operational Global Analysis data) weather data of the selected moments were input into the WRF model as the boundary conditions.

Weather Variable	**Case 1**	**Case 2**
Time	201707241700	202208131800
Daily average temperature at 2m	34.33 ℃	34.33 ℃
Wind speed at 10m	20 km/h	20 km/h
Wind direction at 10m	180° (to north)	260° (to north)

Table 1. Weather conditions representing the two selected cases

3.2. WRF CONFIGURATION

In this study, simulations were carried out using WRF version 4.4 to obtain the required weather variables. We set up five layers of nested areas with the centroid set at the Nanjing Museum location (118.9° E, 30.14° N), applied a scale factor of 3 between each nested domain, with the innermost 40 km * 40 km domain 5 covering the main urban area of Nanjing (Figure 2), and used the Lambert projection suitable for the Northern Hemisphere region. For the urban canopy setting, we used the multilayer urban canopy model BEM (Building Environment Model) adapted for urban-scale microclimate studies (Wang et al., 2019). We also inserted local climate zone (LCZ) classification data from WUDAPT into the surface and canopy geographic files, considering the urban built environment and anthropogenic heat, thereby obtaining more accurate UHI distribution and intensity maps. In addition, we used physical schemes and dynamic parameters suitable for the study. The simulation results revealed the CUHII (Figure 3), which were at the same mean temperature and the same mean wind speed but different wind directions.

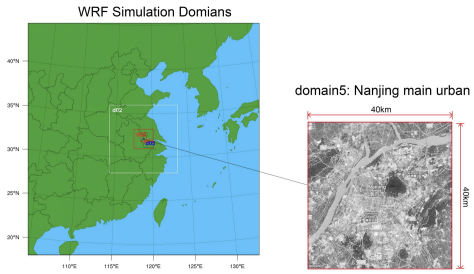

Figure 2. WRF domains

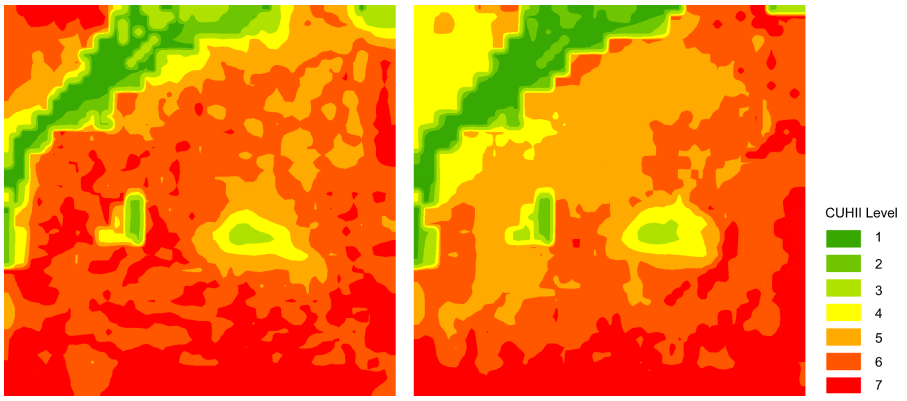

Figure 3. CUHII in case 1 (left) & case 2 (right)

3.3. DATA VERIFICATION

To verify the accuracy of the WRF simulation results, we compared the hourly results of the WRF simulation with the data from the Nanjing observatory and obtained the results. In this case, the temperature accuracy was compared using the T2 (air temperature at 2 m) variable with the temperature measured in the 1.5 m louver box. And the wind conditions obtained by the variables V10 and U10 were compared with the wind condition measured at 10 m. The results showed a high correlation (relevant value of 0.91), which indicates that the results of the multi urban canopy model of WRF used for this study are reliable.

We also compared the WRF simulation results with satellite data for validation. Surface temperature inversions were obtained from Landsat 8 imagery during low cloudiness days in Nanjing, and the results were compared with the variable surface temperature from WRF. The results showed a high correlation, further validating the accuracy of the WRF model in performing weather simulation.

3.4. DATA & STATISTICS

After calculating the canopy temperature and the wind conditions of two comparative weather cases based on the WRF simulation results, an analysis of relevance was carried out. On the one hand, to identify and distinguish CUHIs and their distributions in both weather cases with air temperatures by the natural breakpoint classification method, we compared the wind characteristics in three types of CUHII zones: zone 1 with a high-level CUHII only in weather case 1, zone 2 with a high-level CUHII only in weather case 2, zone 3 with high-level CUHIIs in both weather cases. On the other hand, the increase or decrease of canopy temperature was considered to quantify the CUHI. The "main cooling zone" and "main warming zone" according to the temperature distribution were identified. Then the wind characteristics could be compared in these zones.

4. Results

4.1. CUHII CHANGES AND WIND DIRECTIONS

The distribution of wind direction differed among each CUHII zone when the intensity of heat island changed. We classified the CUHI zones according to the intensity: CUHI Zone 1 that existed only in the first case (CUHII1≥6 and CUHII2≤5), CUHI Zone 2 existed only in the second case (CUHII1≤5 and CUHII2≥6) and CUHI Zone 3 that existed in both cases (CUHII1≥6 and CUHII2≥6) (Figure 4). The statistical values of the wind directions in each case are shown in Table 2, which indicates that in zones where the CUHII changed significantly, the wind direction distribution (Figure 5) was centralized in some intervals and showed a Gaussian distribution, either in the zones where CUHII increased significantly or in zones where the CUHII decreased significantly. Particularly, in the area where the CUHII increased most significantly, the standard deviation of the wind direction value was the smallest, concentrated at approximately 140° (Case 1) and 43° (Case 2).

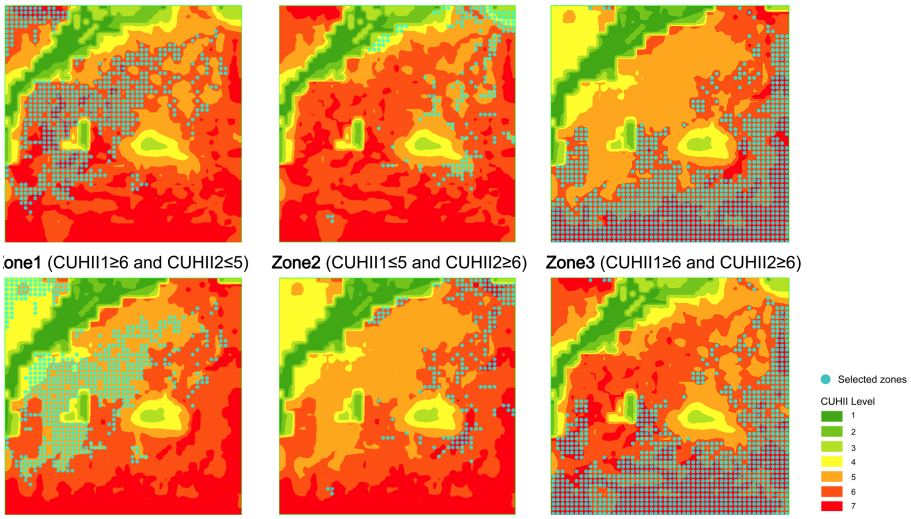

Figure 4. Zone 1, 2 and 3 in cases 1 (top) & case 2 (bottom)

Zone	Zone 1		Zone 2		Zone 3	
Case No.	Case 1	Case 2	Case 1	Case 2	Case 1	Case 2
Direction (average)	112.12°	45.8°	138.9°	43.1°	98.0°	40.0°
Standard deviation	125.8°	14°	19.6°	9.3°	59.3°	30.5°

Table 2. Wind direction statistics in Zone 1, Zone 2 and Zone 3

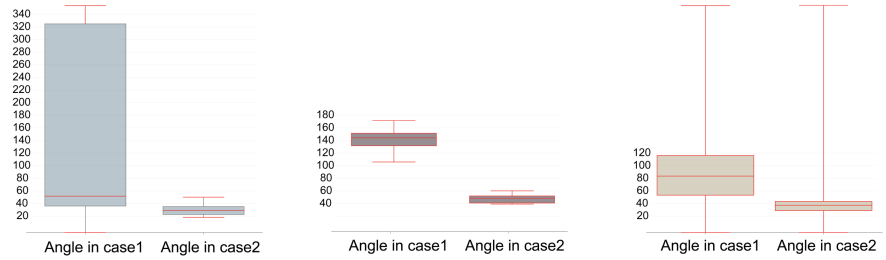

Figure 5. Distributions of the wind directions in Zone 1, 2 and 3

4.2. AIR TEMPERATURE CHANGES AND WIND DIRECTIONS

The distributions of wind directions differed when the air temperature changed. The temperature comparison between the two weather cases indicates that there exists a significant change in temperature in the same area with the same overall average temperature, ranging from -2.8°C to 2.3°C with natural breakpoints at -1.4˚C and 0.8˚C. Therefore, we analyzed the distributions of wind directions in the zones where the temperature changed mostly. First, we identified the "main cooling zones" (-2.8˚C to -1.4˚C) and "main warming zones" (0.8˚C to 2.3˚C) according to the temperature changes (Figure 6). Second, we investigated the distribution of wind directions in these zones, and found that the wind direction distribution was most centralized in the "main warming zones", within the range of 135° (case 1) and 45° (case 2); the wind direction distribution of the "main cooling zones" was centralized at approximately 40° (case 2) (Figure 7).

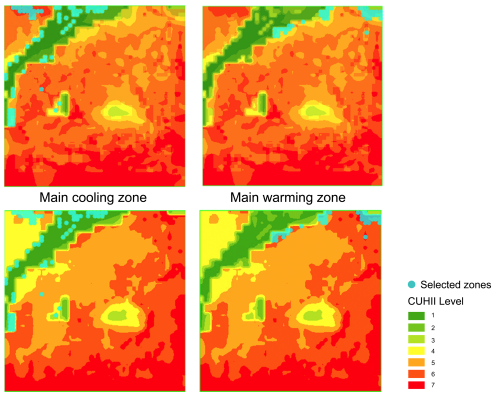

Figure 6. Main cooling zones and main warming zones in case 1 (top) & case 2 (bottom)

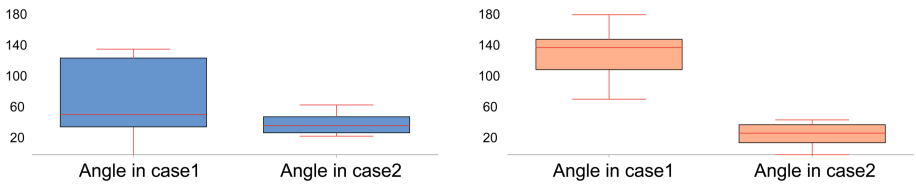

Figure 7. Distributions of wind directions in main cooling zones (left) and main warming zones

(right)

5. Conclusion & Discussion

The main purpose of the study was to investigate the correlation between urban canopy heat islands and wind conditions. Through this study, we achieved the identification and classification of CUHIs, which has received less mainstream research attention in urban heat island. And we developed a technical path to compare multiple variables such as CUHII and wind conditions. In terms of weather cases, the main urban area of Nanjing was chosen as the study area, and the two moments with the highest average daily temperatures in Nanjing were chosen as comparison cases.

The wind directions of zone 3 in both cases and of zone 2 in case 2 were relatively similar, indicating that wind directions at an angle of 50-90° lead to an increased CUHII and maintained it at a high level. This finding suggests that for the main urban area of Nanjing, the presence of wind directions in a particular range is insufficient to mitigate the CUHII, which could lead to a continuous increase in air temperature, causing health risks to urban residents and further increasing the risk of heat exposure.

The comparison of the overall CUHII results in 2 cases showed a relatively large reduction in the CUHI area when the wind directions were within some specific angular intervals. This implies that the wind directions within one or several intervals may have greater impacts on the overall CUHI intensity, which may be related to the specific urban form of the study area or ventilation corridors in the main urban area. When the wind direction changes, the urban ventilation effect is optimized, resulting in a significant decrease in the urban canopy temperature and enhancing public health.

The conclusions presented in the study are somewhat regular in nature, but there is also some variability regarding the overall wind distribution range. The wind direction of zone 1 in case 1 exhibited a large number of outliers and a wide distribution range. The results may have been caused by the specific wind conditions. Therefore, in the follow-up study, we will consider selecting more meteorological cases to improve the reliability of the research data, such as choosing other extremely hot days, filtering error values during data processing, and incorporating more cases with various wind conditions. These extended studies will build on the current findings and continue our exploration of the possible existence of further patterns.

Furthermore, the identification of CUHIs and their relationships with wind conditions can help to predict the times, locations, and durations of local high temperature zones during extreme heat days. This can thus effectively reduce the risk of heat exposure for urban dwellers when living and working and will help provide suggestions for urban management, public health, and related policymaking.

References

Chen, B., Xie, M., Feng, Q., Wu, R. & Jiang, L. (2022). Diurnal heat exposure risk mapping and related governance zoning: A case study of Beijing, China. Sustainable Cities and Society, 81, 103831, DOI:10.1016/j.scs.2022.103831.

Estoque, R. C., Ooba, M., Seposo, X. T., Togawa, T., Hijioka, Y., Takahashi, K. & Nakamura, S. (2020). Heat health risk assessment in Philippine cities using remotely

sensed data and social-ecological indicators. Nature Communications, 11(1), 1581, https://doi.org/10.1038/s41467-020-15218-8.
He, B.-J. (2022). Climate Change and Environmental Sustainability. Advances in Science, Technology & Innovation, 131–136.
Hu, Y., Hou, M., Jia, G., Zhao, C., Zhen, X. & Xu, Y. (2019). Comparison of surface and canopy urban heat islands within megacities of eastern China. ISPRS Journal of Photogrammetry and Remote Sensing, 156(11), 160–168, DOI:10.1016/j.isprsjprs.2019.08.012.
Huang, F., Zhan, W., Wang, Z.-H., Voogt, J., Hu, L., Quan, J., Liu, C., Zhang, N. & Lai, J. (2020). Satellite identification of atmospheric-surface-subsurface urban heat islands under clear sky. Remote Sensing of Environment, 250, 112039, https://doi.org/10.1016/j.rse.2020.112039.
Li, B., Zhang, B., Yin, L. & Chang, J. (2023). Assessing heat risk for residents of complex urban areas from an accessibility-based perspective. Sustainable Cities and Society, 88(Forest Ecology and Management 446 2019), 104278, https://doi.org/10.1016/j.scs.2022.104278.
Liang, Z., Wu, S., Wang, Y., Wei, F., Huang, J., Shen, J., & Li, S. (2020). The relationship between urban form and heat island intensity along the urban development gradients. The Science of the total environment, 708, 135011. https://doi.org/10.1016/j.scitotenv.2019.135011
Lu, Y., He, T., Xu, X. & Qiao, Z. (2021). Investigation the Robustness of Standard Classification Methods for Defining Urban Heat Islands. IEEE Journal of Selected Topics in Applied Earth Observations and Remote Sensing, 14, 11386–11394, doi: 10.1109/JSTARS.2021.3124558.
Peng, W., Wang, R., Duan, J., Gao, W. & Fan, Z. (2022). Surface and canopy urban heat islands: Does urban morphology result in the spatiotemporal differences? Urban Climate, 42, 101136, DOI:10.1016/j.uclim.2022.101136.
Thanvisitthpon, N. (2023). Statistically Validated Urban Heat Island Risk Indicators for UHI Susceptibility Assessment. International Journal of Environmental Research and Public Health, 20(2), 1172, https://doi.org/10.3390/ijerph20021172.
Wang, T. (2019). Research on Urban Morphology Modelling and Numerical Simulation of Microclimate Based on Local Climate Zones at Macro Scale [Master's thesis, Nanjing University].
Wang, W., Yao, X. & Shu, J. (2020). Air advection induced differences between canopy and surface heat islands. Science of The Total Environment, 725, 138120, DOI: 10.1016/j.scitotenv.2020.138120.
Xue, J., Zong, L., Yang, Y., Bi, X., Zhang, Y. & Zhao, M. (2023). Diurnal and interannual variations of canopy urban heat island (CUHI) effects over a mountain–valley city with a semi-arid climate. Urban Climate, 48, 101425, https://doi.org/10.1016/j.uclim.2023.101425.
Zheng, Z., Ren, G., Gao, H. & Yang, Y. (2022). Urban ventilation planning and its associated benefits based on numerical experiments: A case study in beijing, China. Building and Environment, 222, 109383, https://doi.org/10.1016/j.buildenv.2022.109383.
Zhou, Y., Zhao, H., Mao, S., Zhang, G., Jin, Y., Luo, Y., Huo, W., Pan, Z., An, P. & Lun, F. (2022). Exploring surface urban heat island (SUHI) intensity and its implications based on urban 3D neighborhood metrics: An investigation of 57 Chinese cities. Science of The Total Environment, 847, 157662, https://doi.org/10.1016/j.scitotenv.2022.157662.